Lymphocyte migration and retention properties affected by ibrutinib in chronic lymphocytic leukemia

Javier Rey-Barroso,[1°] Alice Munaretto,[1+] Nelly Rouquié,[1+] Aurélie Mougel,[1] Malika Chassan,[2] Sébastien Gadat,[3,4] Océane Dewingle,[5°] Renaud Poincloux,[6] Sarah Cadot,[5] Loïc Ysebaert,[5,7] Anne Quillet-Mary[5] and Loïc Dupré[1,8]

[1]Toulouse Institute for Infectious and Inflammatory Diseases (INFINITy), INSERM, CNRS, Toulouse III Paul Sabatier University, Toulouse, France; [2]Institut de Mathématiques de Toulouse, CNRS UMR 5219, Université Toulouse 3 Paul Sabatier, Toulouse, France; [3]Toulouse School of Economics, CNRS UMR 5314, Université Toulouse 1 Capitole, Toulouse, France; [4]Institut Universitaire de France, Paris, France; [5]Toulouse Cancer Research Center (CRCT), INSERM, CNRS, Toulouse III Paul Sabatier University, Toulouse, France; [6]Institut de Pharmacologie et Biologie Structurale, IPBS, CNRS, UPS, Université de Toulouse, France; [7]Clinical Hematology, IUCT Oncopole, Toulouse University Hospital, Toulouse, France and [8]Department of Dermatology, Medical University of Vienna, Vienna, Austria

[+]*AM and NR contributed equally.*

[°]*Current address: Institut de Pharmacologie et Biologie Structurale, IPBS, CNRS, UPS, Université de Toulouse, Toulouse, France.*

Lymphocyte migration and retention properties affected by ibrutibnib in Chronic Lymphocytic Leukemia

by Javier Rey-Barroso et al.

Supplementary material content

Supplementary Methods

Chemokine-evoked migration upon in vitro exposure to ibrutinib

Frozen PBMCs samples from CLL patients or healthy donors were thawed in RPMI 1640 GlutaMax, supplemented with 10% Fetal Calf Serum medium (RPMI-10% FCS) and let rest for 1 h at 37°C. Then, 50.000 cells were seeded in the upper compartments of Transwell-96 well plates (Corning) with a pore size of 5 μm in the presence or absence of 500 nM ibrutinib. The lower chamber of the wells was filled with RPMI-10% FCS medium containing 1000 ng ml^{-1} CCL19, 500 ng ml^{-1} CXCL12 or 1000 ng ml^{-1} CXCL13. Medium without chemokine was used as a control for basal migration. After 6 h of incubation, migrated cells present on the lower chamber of the wells were stained 30 min at 4°C with anti-CD3 and anti-CD19 antibodies, as well as with anti-CD56 antibodies in the case of healthy donors. Then, 100 μl was retrieved from the lower chambers and analyzed on a MACSQuant Q10 cytometer (Miltenyi) to extract total cell counts and proportions of CD3$^+$, CD19$^+$ and CD56$^+$ subsets using the MACSQuantify Software (Miltenyi). Migration for each subset was calculated as percentage to positive control wells in which cells were seeded directly in the lower chamber.

Chemokine-evoked migration during the course of ibrutinib treatment

Frozen PBMCs samples from CLL patients from the CompuTreatCLL cohort before and after 1, 3 and 6 months of ibrutinib treatment were thawed in RPMI-10% FCS medium and let rest for 1 h at 37°C. Then, 50.000 cells were seeded in the upper compartments of Transwell-96 well plates (Corning) with a pore size of 5 μm. The lower chamber of the wells was filled with RPMI-10% FCS medium containing 1000 ng ml^{-1} CCL19, 500 ng ml^{-1} CXCL12 or 1000 ng ml^{-1} CXCL13.

Medium without chemokine was used as a control for basal migration. After 6 h of incubation, migrated cells present on the lower chamber of the wells were stained 30 min at 4°C with anti-CD3 and anti-CD19 antibodies and analyzed using the procedure described above.

Live recording of basal and chemokine-evoked cell motility

PBMCs from CLL patients were cultured at 5×10^6 cells ml^{-1} in RPMI-10% FCS supplemented with 5 μM CpG ODN 2006 (InvivoGen) and 100 IU ml^{-1} human recombinant IL-2 (Peprotech) for 48 h. Cells were pre-incubated 30 min at 37°C with anti-CD3-PE antibody in order to distinguish T cells from CLL cells. Then, 100.000 cells resuspended in RPMI-10% FCS in the presence or absence of 500 nM ibrutinib were seeded in each channel of a μ-Slide VI 0.4 slide (Ibidi) coated with 5 μg ml^{-1} fibronectin. After 3 h, cells were imaged for a 12-h period at 37 °C and 5% CO_2 using on a Zeiss apotome microscope, collecting red and bright field channels with a 10x/0.45 NA objective. T cell position was identified using red channel, then subtracted via image treatment on the bright field channel in order to extract CLL cell positions. Tracks were quantified using the image J plugin Trackmate for both cell types. Tracks of at least 20 min and a minimum displacement of 10 μm were selected for speed measurements. For chemokine evoked motility experiments, CCL19 was added to the medium at 500 ng ml^{-1}.

Migration along CCL19 gradients

PBMCs from CLL patients were cultured at 5×10^6 cells ml^{-1} in RPMI-10% FCS supplemented with 5 μM CpG ODN 2006 (InvivoGen) and 100 IU ml^{-1} human recombinant IL-2 (Peprotech) for 48 h. Cells were pre-incubated 30 min at 37°C with anti-CD3-PE antibody in order to distinguish T cells from CLL cells. Then, 50.000 cells resuspended in RPMI-10% FCS in the

presence or absence of 500 nM ibrutinib or acalabrutinib were loaded into the central transversal channel of ibitreat 3D chemotaxis μ-slides (Ibidi) coated with 5 μg ml^{-1} fibronectin and incubated at 37 °C for 30 min to allow cell attachment. Then, 0–500 ng ml^{-1} CCL19 gradients were set following the manufacturer's instructions. Gradient linearity was verified with a 10% dextran-FITC solution. Cell migration was assessed by recording 1 image of red and bright field channels per min for 14 h with an Apotome microscope (Zeiss) and a 5X / 0.15 NA objective in temperature and CO_2 controlled conditions. As previously described, CLL and T cell tracks were isolated by image treatment and quantified using the image J plugin Trackmate. Tracks of at least 20 min and a minimum displacement of 10 μm were selected for speed measurements. Chemotaxis plots and migration parameters (FMI-Y and total speed) were obtained using the Chemotaxis and Migration tool from Ibidi.

Morphological analysis of ibrutinib-exposed CLL cells by high-content cell imaging

PBMCs from CLL patients were cultured at 5×10^6 cells ml^{-1} in RPMI-10% FCS supplemented with 5 μM CpG ODN 2006 (InvivoGen) and 100 IU ml^{-1} human recombinant IL-2 (Peprotech) for 48 h. BTK phosphorylation and morphological descriptors were analyzed in parallel in CLL cells from multiple patients upon in vitro ibrutinib exposure using a recently developed high-content cell imaging platform adapted to the study of lymphoid cell populations[1]. Briefly, 384-well PhenoPlates (PerkinElmer) were coated with either 0.1 mg ml^{-1} poly-L-lysine, 2 μg ml^{-1} recombinant human ICAM-1-Fc chimera (R&D Systems), 10 μg ml^{-1} anti-BCR antibodies or a combination of ICAM-1 and anti-BCR antibodies. CLL patient cells were seeded at 10.000 cells per well (3 replicates per condition) and incubated for 15 min at 37°C in the presence or absence of 500 nM ibrutinib. Cells were fixed by adding a small volume of 16% paraformaldehyde (3%

final concentration) 15 min at 37°C. They were then permeabilized in permeabilization buffer (eBioscience) and stained with AlexaFluor488-conjugated anti-CD19 antibodies, phalloidin-AlexaFluor555 (ThermoFisher Scientific), AlexaFluor647-conjugated anti-phospho-BTK antibodies (BD Biosciences) and DAPI. An anti-CD18 antibody (TS1/18) was used to assess whether the spreading upon ICAM-1/anti-BCR antibody stimulation was dependent on the engagement of LFA-1. The specificity of the phospho-BTK staining was verified by using an isotype antibody. Images were acquired on an automated spinning disk confocal device (Opera Phenix, PerkinElmer) equipped with a 40x 1.1 NA Plan Apochromat water immersion objective and sCMOS cameras (16 bits, 2160 × 2160 pixels, 6.5 μm pixel size). Image datasets were processed with Harmony software (PerkinElmer) to extract phospho-BTK intensity, cell area and F-actin texture from the CD19^{+} CLL cells at the confocal plane corresponding to the cell to substrate interface.

Scanning electron microscopy imaging

Following exposure to 500 nM ibrutinib ibrutinib for 30 min, were seeded for 30 min on coverslips coated with PLL or ICAM-1 + anti-BCR antibody, then fixed for 10 min in a 0.2 M sodium cacodylate buffer (pH 7.4) containing 2% paraformaldehyde (Electron Microscopy Sciences 15710) and 2.5% glutaraldehyde (Electron Microscopy Sciences 16220), then washed with distilled water. Samples were dehydrated through a graded series (25–100%) of ethanol, transferred in acetone and subjected to critical point drying with CO_2 in a Leica EM CPD300. Samples were then sputter-coated with 3 nm platinum with a Leica EM MED020 evaporator. They were examined and photographed with an FEI Quanta FEG250 electron microscope.

Flow cytometry bar coding for longitudinal analysis of surface receptors in leukemic cells and T cells

PBMCs from CLL patients, that had been collected and frozen along the course of ibrutinib treatment, were thawed and counted. For each of the 5 time points (0, 1, 2, 3 and 6 months after treatment initiation), samples were labeled with a specific concentration (0, 0.04, 0.2, 1 and 3 μM, respectively) of CellTrace™ Violet (Invitrogen) during 20 min at 37°C. Barcoded samples were washed, pooled and labeled with Fixable Viability Dye-eFluor780 (Affymetrix eBioscience) during 15 min at 4°C. The viability of the tested samples was between 90 and 97%. Pooled barcoded samples were stained 30 min at 4°C for extracellular markers with antibodies listed in **Suppl Table S1**. Samples were subsequently fixed with 2% paraformaldehyde and stained 30 min at 4°C for intracellular markers with antibodies listed in **Suppl Table S1**. Data were acquired on a BD FACSCalibur cytometer and analyzed using Flowjo software, by separating the different longitudinal samples on the basis of the CTV staining.

Reference

1   German Y, Vulliard L, Kamnev A, et al. Morphological profiling of human T and NK
        lymphocytes by high-content cell imaging. Cell Rep. 2021;36(1):109318.

**Table S1. Antibodies used for flow cytometry bar coding analysis**

| Marker	Fluorochrome	Clone	Producer	Reference	Panels								
					1	2	3	5	6	7	8	9	10
CTV (bar coding)			Invitrogen	C34557	x	x	x	x	x	x	x	x	x
Live/dead	eFluor780		Affymetrix eBioscience	65-0865	x	x	x	x	x	x	x	x	x
CD19	BV510	SJ25-C1	BD Biosciences	562953		x	x	x	x	x	x		
CD5	A700	UCHT2	BD Biosciences	561159		x	x	x	x	x	x		
CD3	PE-Cy7	UCHT1	BD Biosciences	563423		x	x	x	x	x	x	x	x
CD4	FITC	RPA-T4	BD Biosciences	555346		x	x	x	x	x	x	x	x
CD8	BV786	RPA-T8	BD Biosciences	563823		x	x	x	x	x	x	x	x
S1PR	eFluor660	SW4GYPP	eBioscience	50-3639		x							
CCR7	PE	150503	BD Biosciences	560765		x							
CXCR4	PE-CF594	12G5	BD Biosciences	562389		x							
CXCR3	PE-Cy5	1C6	BD Biosciences	561731			x						
CXCR5	PE	51505	R&D System	FAB190P-02			x						
CCR5	PE-CF594	2D7	BD Biosciences	562456			x						
LFA-1	BV650	HI111	BD Biosciences	563934			x						
LAG-3	PE	T47-530	BD Biosciences	565617					x				
BTLA	PE-CF594	J168-540	BD Biosciences	564801					x				
CD69	BV650	FN50	BD Biosciences	563835					x				
VLA-4	PE-Cy5	9F10	BD Biosciences	559880					x				
CD11c	BV650	B-ly6	BD Biosciences	563403						x			
CD276	PE	DCN.70	Biolegend	331606						x			
CD44	PE-CF594	G44-26	BD Biosciences	562818						x			
ICAM-1	PE-Cy5	HA58	BD Biosciences	555512						x			
LFA-3	PE-Cy5	1C3	BD Biosciences	551399							x		
Perforin*	PE-CF594	dG9	BD Biosciences	563763							x		
Granzyme B*	PE	REA226	Miltenyi Biotec	130-101-351							x		
LAMP-1*	BV650	H4A3	Biolegend	328637							x		
CD45RA	A700	HI100	BD Biosciences	560673									x
CD45RO	BV510	UCHL1	BD Biosciences	563215									x
CCR7	PE	150503	BD Biosciences	560765									x
CD27	BV650	L128	BD Biosciences	563229									x
CD137	PE-Cy5	4-1BB	BD Biosciences	551137									x
CD57	FITC	NK-1	BD Biosciences	562488									x

*Intracellular staining
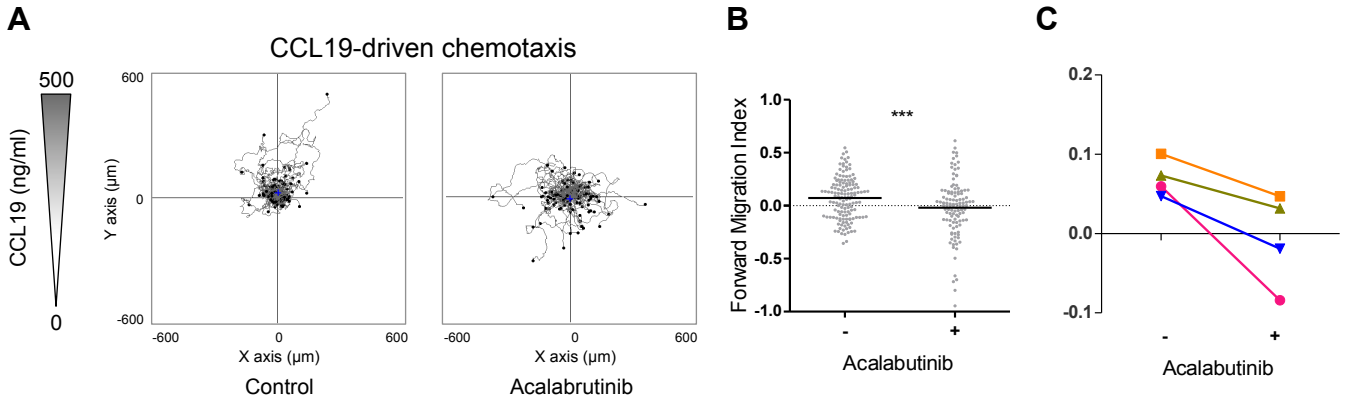
Supplementary Figure S1. Acalabrutinib impairs the directional migration of CLL cells along CCL19 gradients. (**A**) Control or acalabrutinib treated PBMCs were seeded on fibronectin, exposed to a CCL19 chemokine gradient and imaged. Panels show tracks of control and ibrutinib treated CLL cells. (**B**) Forward Migration Index along the CCL19 gradient (Y axis) of cells tracked in A. Values for individual cells and mean are represented. Mann-Whitney test was applied. (**C**) Forward Migration Index along the CCL19 gradient (Y axis) of cells from 4 CLL patients (mean values). Two-ways ANOVA (mixed model) and Bonferroni multiple test were applied and shown statistically significant differences for 4 out of 4 patients.
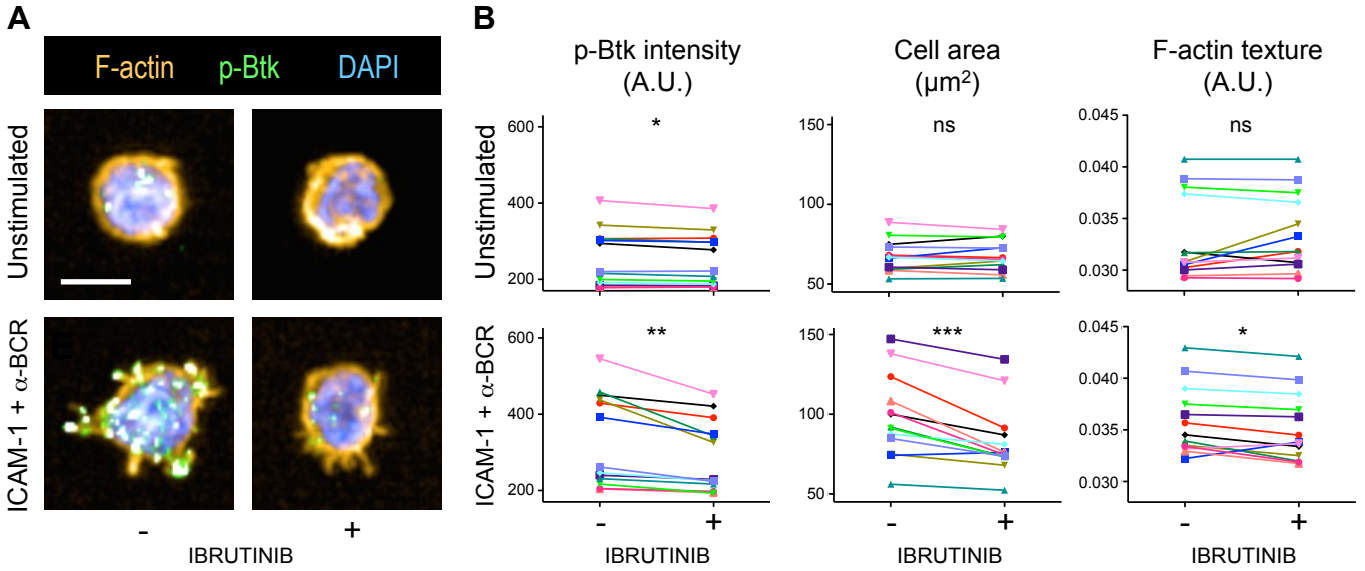
Rey-Barroso *et al.*

A
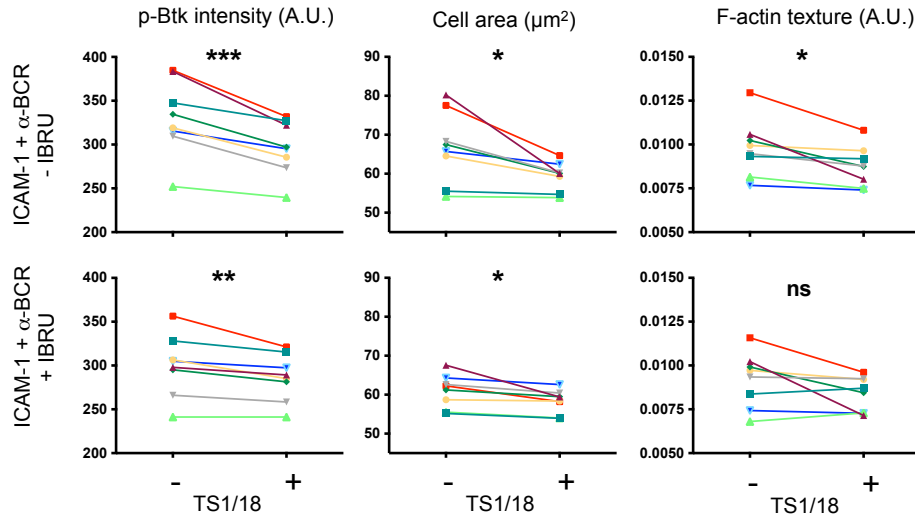
Supplementary Figure S2. Contribution of the ICAM-1-LFA-1 axis to CLL immunological synapse assembly.
(**A**) Following automated recognition of individual cells based on the DAPI and F-actin staining, p-BTK intensity, cell area and F-actin texture were quantified for each cell. N>100 cells/condition. Mean parameter values for 8 patients as in Figure 2. Wilcoxon matched-pairs signed rank tests were applied to estimate the statistical significance of anti-LFA-1 (TS1/18) antibody inhibition.
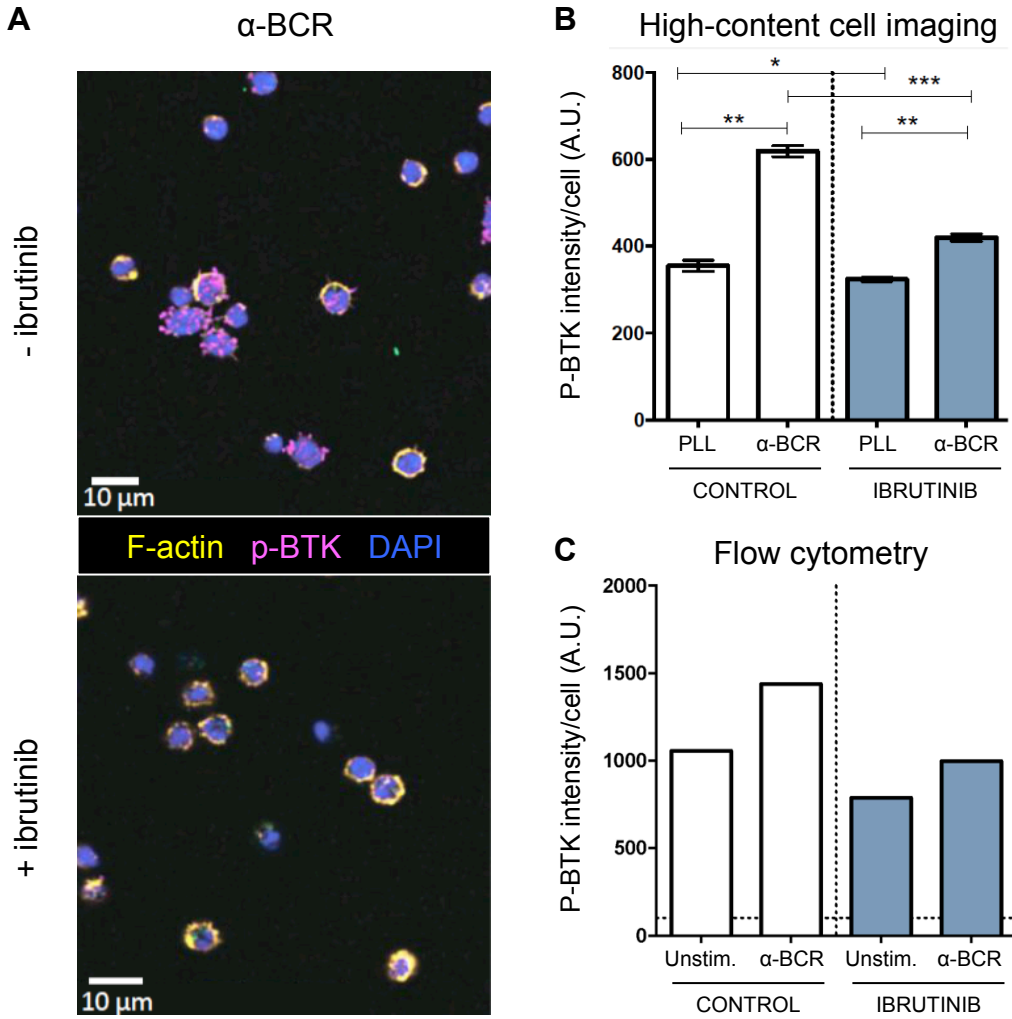
Supplementary Figure S3. Ibrutinib abrogates BCR-evoked BTK phosphorylation in CLL patients. (**A**) Representative confocal images of unexposed and ibrutinib-exposed treated PBMCs, stimulated with coated anti-BCR Ab and stained for F-actin, phosphorylated BTK and DAPI. (**B**) Confocal images were exploited to extract phosphorylated BTK intensity values in cells treated and stimulated in the indicated conditions. One way ANOVA with Bonferroni Multiple Comparison tests were applied (**C**) Parallel analysis of phosphorylated BTK intensity by flow cytometry.

Rey-Barroso *et al.*

Supplementary Figure S4. In vitro exposure to ibrutinib impairs immunological synapse assembly.
(**A**) Representative images of CLL cells stained for F-actin, phosphorylated BTK and DAPI, and imaged on an automated confocal microscope. (**B**) Following automated recognition of individual cells based on the DAPI and F-actin staining, p-BTK intensity, cell area and F-actin texture were quantified for each cell. N>100 cells/condition. Mean parameter values for 13 patients are shown. Wilcoxon matched-pairs signed rank tests were applied to estimate the statistical significance of ibrutinib inhibition.

A

CONTROL   IBRUTINIB

B
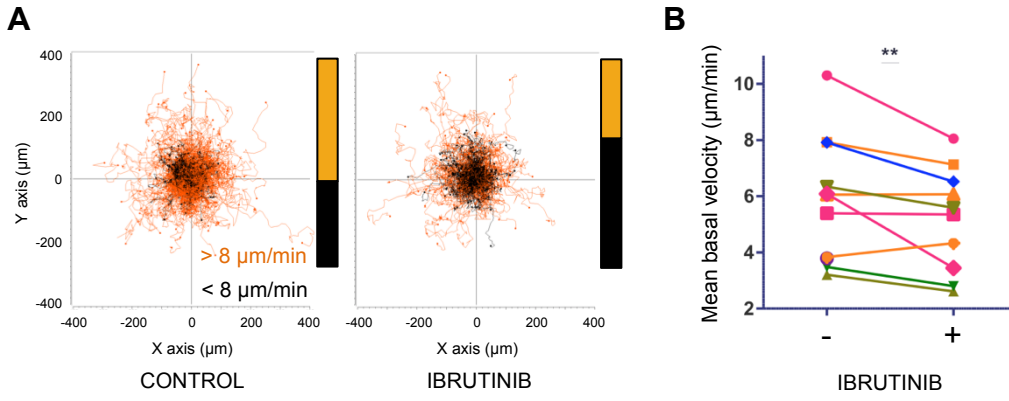
IBRUTINIB

Supplementary Figure S5. Ibrutinib reduces the velocity of T cells from CLL patients over fibronectin. (**A**) Control or ibrutinib treated PBMCs were seeded on fibronectin and T cells were tracked by live imaging. Panels show 2 h tracks, color-coded using a 8 μm min^{-1} threshold for mean speed; bar on the right summarizes the proportion of cells over (orange) and under (black) the threshold. (**B**) Comparison of mean basal velocity between control and ibrutinib treated samples. N=10 patients. Wilcoxon matched-pairs signed rank tests was applied.
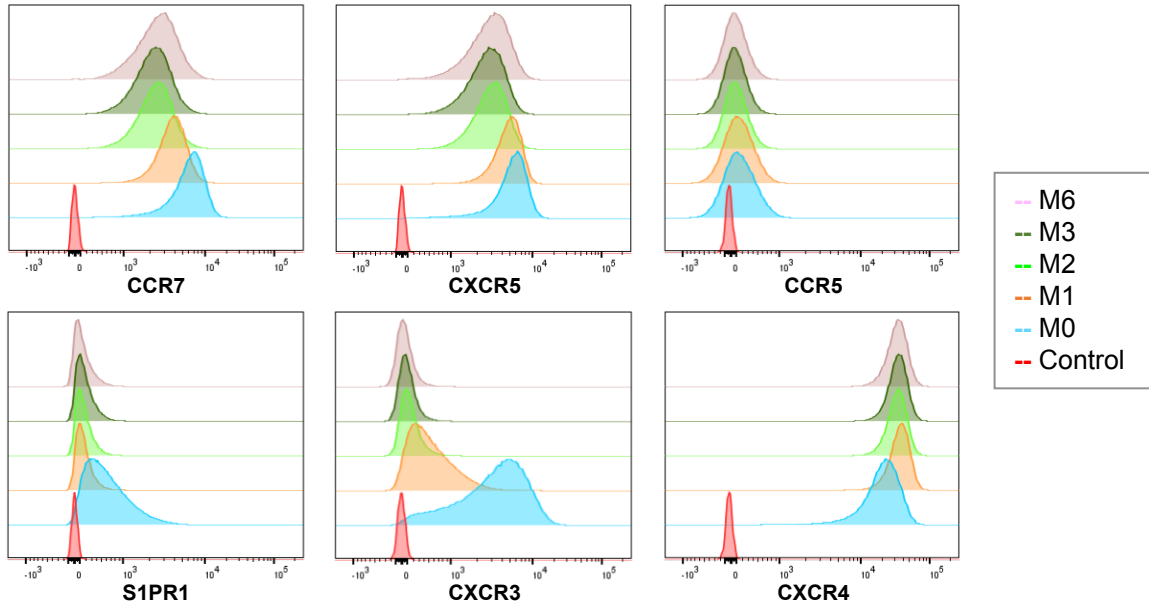
Rey-Barroso *et al.*
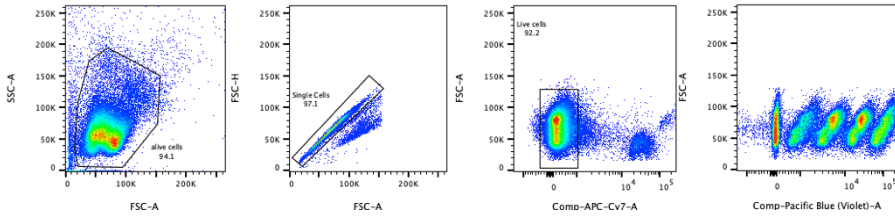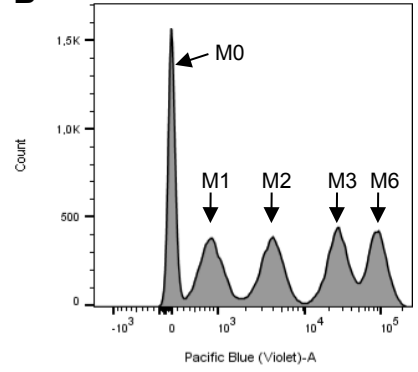
Supplementary Figure S6. Flow cytometry bar-coding strategy for the longitudinal assessment of CLL and T cell receptor expression. (**A**) Gating strategy used to analyse pooled CLL PBMC samples after prestaining with different Pacific Blue dye dilutions. (**B**) Histogram representation of the pooled samples (M0: pre-treatment, M1-6: months post treatment initiation). (**C**) Expression along the course of ibrutinib treatment of the indicated motility receptors in gated CLL leukemic cells from one representative patient.
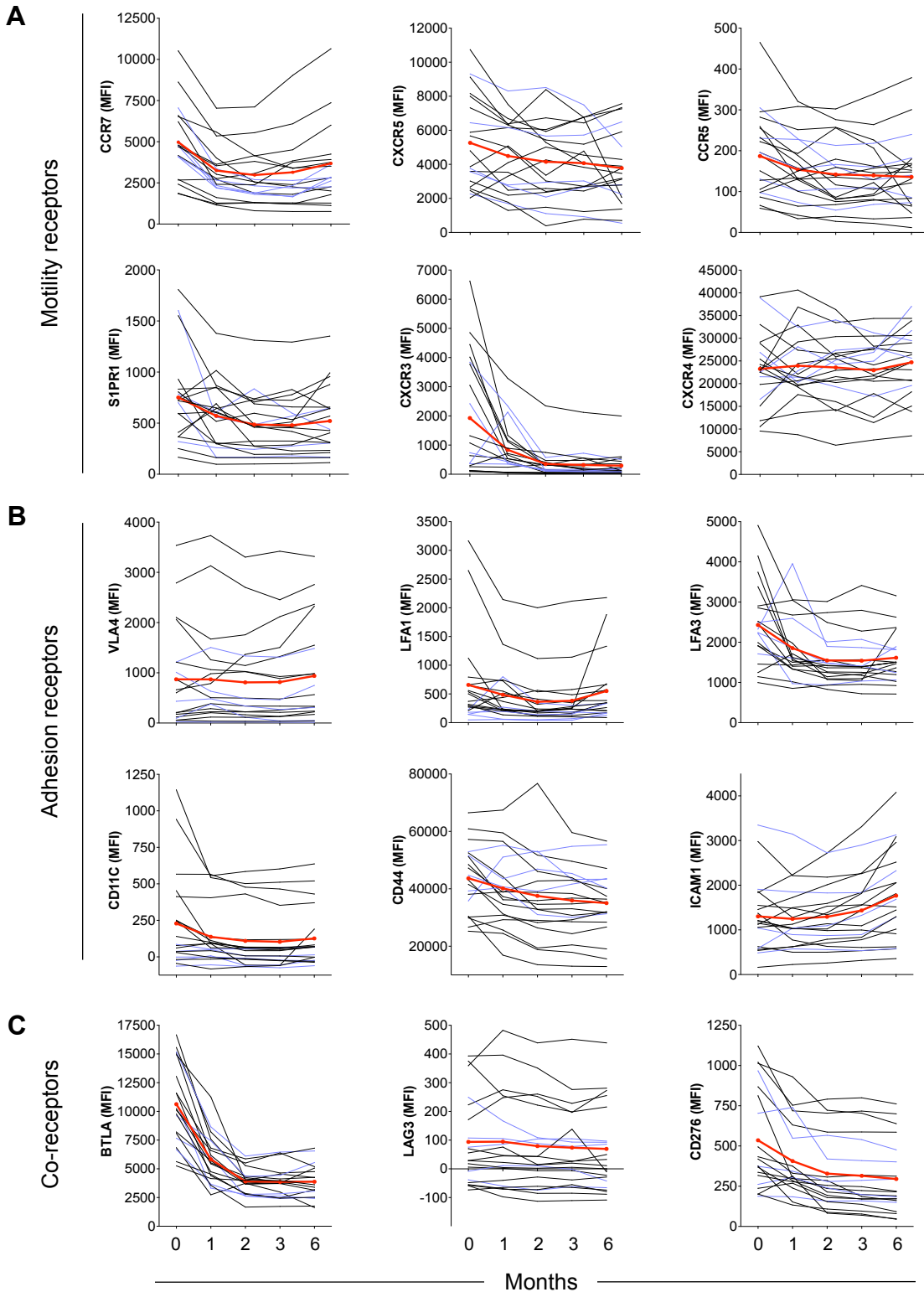
Supplementary Figure S7. Kinetics of surface receptor expression as a function of LFA-1 expression status in CLL patients treated with ibrutinib. (**A**) Longitudinal evolution of the expression of the indicated receptors as MFI on CLL leukemic cells of patients with residual LFA-1 expression (black lines) or negative LFA-1 expression (blue lines) and as a mean of all patients (red lines). (**B**) The indicated adhesion receptors were studied with the same approach as in (A). (**C**) The indicated co-receptors were studied with the same approach as in (A). Two-ways ANOVA (mixed model) and Bonferroni multiple test were applied, not showing statistically significant differences between LFA-1 subgroups.

Rey-Barroso *et al.*
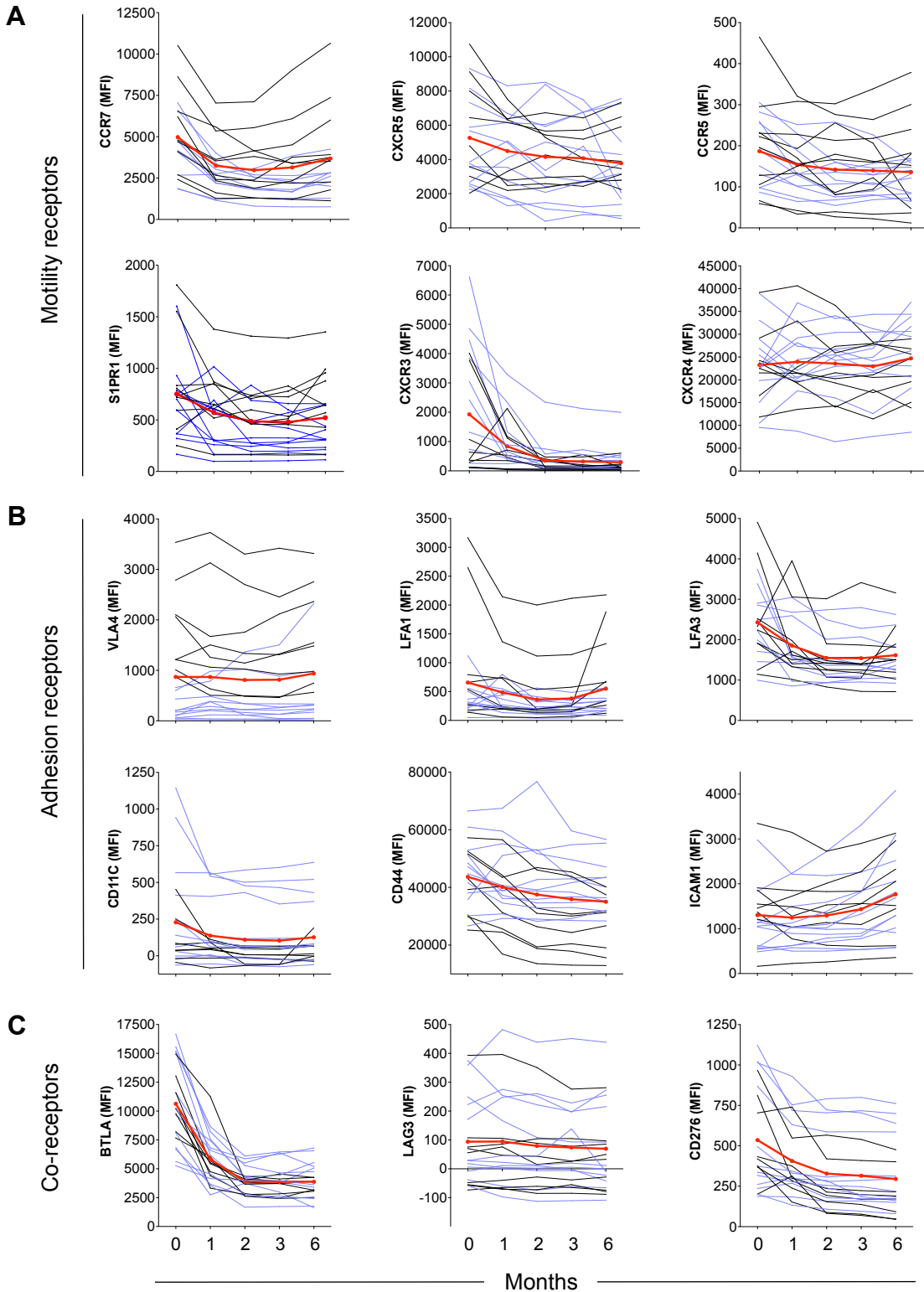
Supplementary Figure S8. Kinetics of surface receptor expression as a function of VLA-4 expression status in CLL patients treated with ibrutinib. (**A**) Longitudinal evolution of the expression of the indicated receptors as MFI on CLL leukemic cells of patients with residual VLA-4 expression (black lines) or negative VLA-4 expression (blue lines) and as a mean of all patients (red lines). (**B**) The indicated adhesion receptors were studied with the same approach as in (A). (**C**) The indicated co-receptors were studied with the same approach as in (A). Two-ways ANOVA (mixed model) and Bonferroni multiple tests were applied, showing statistically significant differences in CD44 expression at months 2, 3 and 6 of treatment between VLA-4 subgroups.
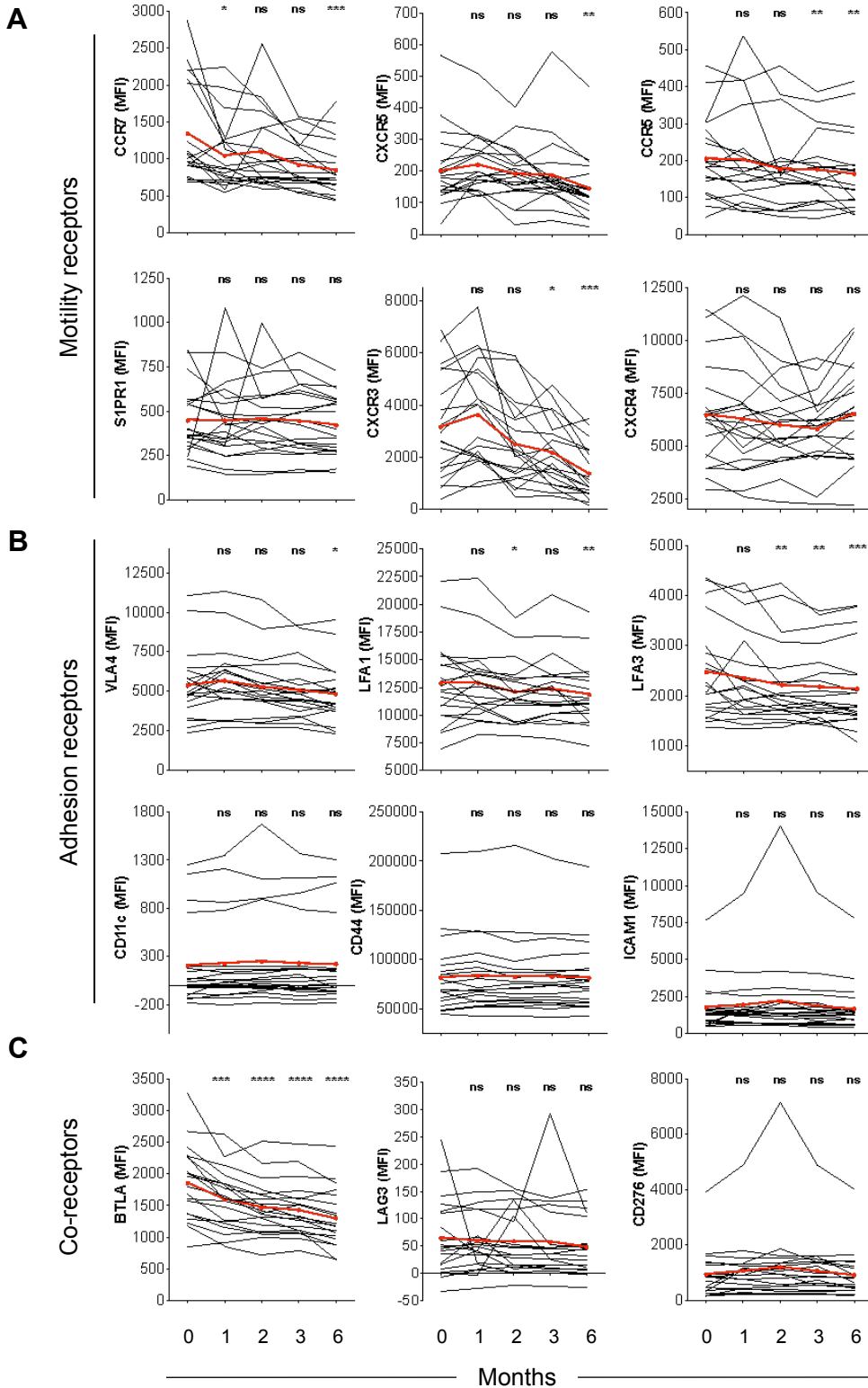
Supplementary Figure S9. Ibrutinib treatment affects differentially the expression of chemokine receptors, adhesion molecules and activation markers in CD4+ T cells. (**A**) PBMCs from 20 CLL patients were collected before and at 1, 2, 3 and 6 months after ibrutinib treatment initiation. The 5 longitudinally collected and frozen samples were thawn together, pre-stained with distinct concentrations of CellTrace™ Violet, mixed in a single tube and stained with antibodies specific of the indicated motility receptors. Data represent the longitudinal evolution of the expression of the indicated receptors on CD4+ T cells as MFI for each patient (black dots and lines) and as a mean (red dots and lines). Friedman test with Dunn's Multiple Comparison tests were applied to estimate the statistical significance of the impact of ibrutinib treatment as compared to the pre-treatment values. (**B**) The indicated adhesion receptors were studied with the same approach as in (A). (**C**) The indicated co-receptors were studied with the same approach as in (A).

Rey-Barroso *et al.*
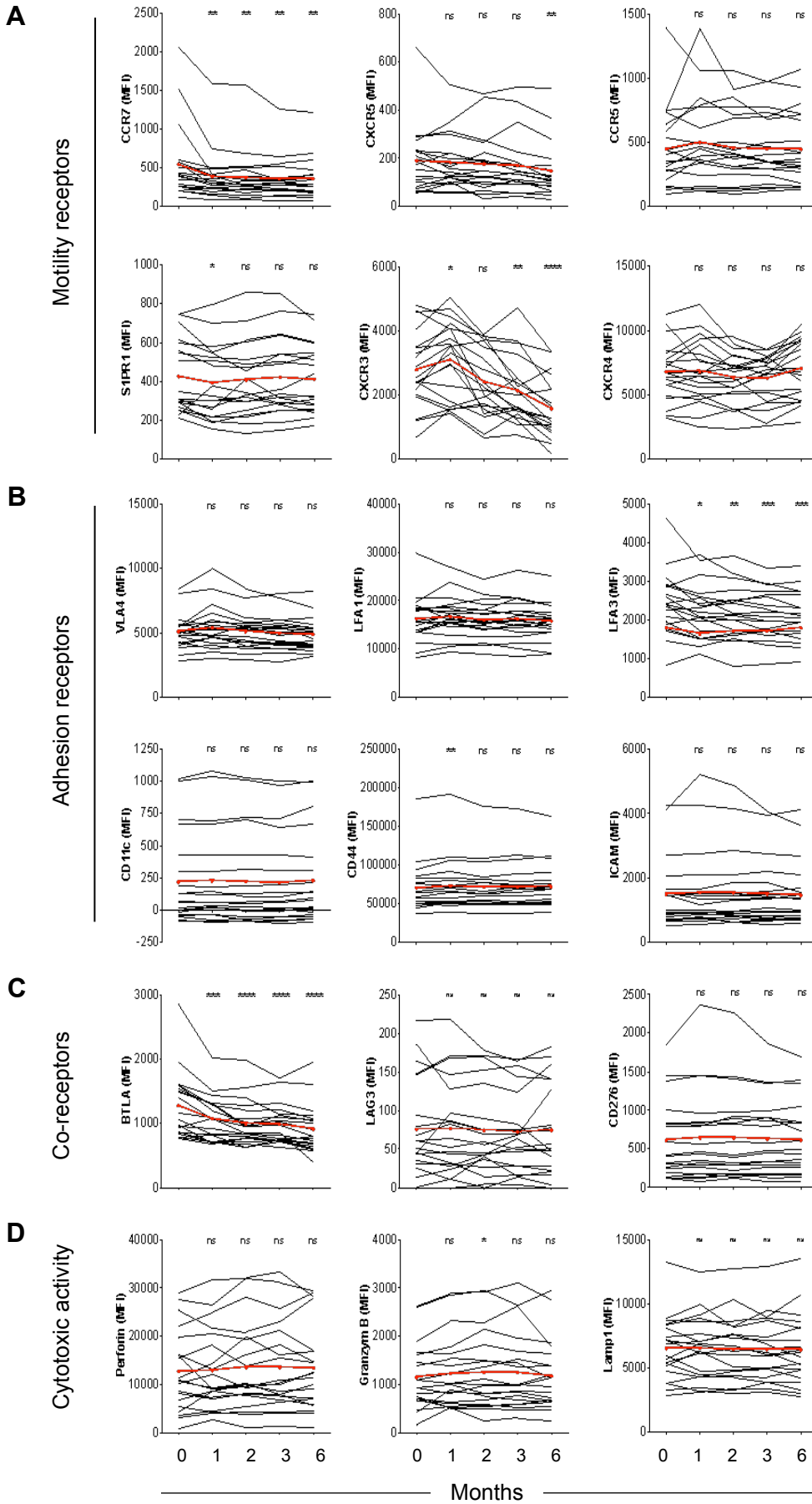
Supplementary Figure S10. Ibrutinib treatment affects differentially the expression of chemokine receptors, adhesion molecules and activation markers in CD8$^+$ T cells. (**A**) PBMCs from 20 CLL patients were collected before and at 1, 2, 3 and 6 months after ibrutinib treatment initiation. The 5 longitudinally collected and frozen samples were thawn together, pre-stained with distinct concentrations of CellTrace™ Violet, mixed in a single tube and stained with antibodies specific of the indicated motility receptors. Data represent the longitudinal evolution of the expression of the indicated receptors on CD8$^+$ T cells as MFI for each patient (black dots and lines) and as a mean (red dots and lines). Friedman test with Dunn's Multiple Comparison tests were applied to estimate the statistical significance of the impact of ibrutinib treatment as compared to the pre-treatment values. (**B**) The indicated adhesion receptors were studied with the same approach as in (A). (**C**) The indicated co-receptors were studied with the same approach as in (A). (**D**) The indicated cytotoxicity-related molecules were studied with the same approach as in (A).